Analyses of Moving Dynamic Loads on Highway Pavements: Part II – Pavement Response

Brian D. Brademeyer[1] **Norbert J. Delatte**[1] **Michael J. Markow**[1]

ABSTRACT

The characterization of the effects of moving, dynamic vehicle loads on pavement deterioration is of fundamental concern to the highway industry. This paper begins by reviewing the mathematical description of vehicle-pavement interaction for different vehicle loading representations. Most of the pavement predictive models in use today do not account for the effects of moving, dynamic loads; therefore, the theoretical concepts required to include the effects of moving, dynamic loads are developed.

The modification of VESYS IIIA to model moving, dynamic single and tandem axle loads on flexible pavements is described. The modified model was verified through a simulation of 23 sections of the AASHO Road Test, and strong correlation was found between model predictions and the Road Test measured damages. This methodology may be applied to a wide range of vehicle configurations. Although the analyses are limited to flexible pavements, the approach will be extended to rigid pavements in the future.

INTRODUCTION

Current models of vehicle-pavement interaction employ simplified models of vehicle loading, such as static or pseudo-moving loads. However, instantaneous dynamic vehicle loads may be considerably higher than static loads (1,2), and thus dynamic loading can have a considerable impact on pavement performance (3). Current models cannot account for this effect. The prediction of pavement deterioration and serviceability under dynamic vehicle loading becomes particularly important when pavement design and analysis methods must be extended to encompass expanding vehicle and pavement technology. The purpose of this paper is to develop a generalized methodology to analyze pavement responses to moving, dynamic vehicle loads, which may be used to predict pavement performance.

DYNAMIC VEHICLE-PAVEMENT INTERACTIONS

The interaction between vehicle loads and pavement responses is frequently characterized as a one-way interaction, wherein the vehicle loads influence pavement responses but not vice versa. In reality, the roughness of the pavement surface induces dynamic forces within the vehicle, which alter the tire forces experienced by the pavement. These dynamic tire forces alter the pavement's primary responses (stresses and strains), which affect the amount of distress or damage produced by the vehicle, which in turn affects the dynamic tire forces produced by subsequent vehicles.

To isolate the various mechanisms involved in these vehicle-pavement dynamics, a formal framework is needed to analyze the progression of damage within a pavement structure, by linking its primary and ultimate response behaviors--a primary response model and a cumulative damage model--together with a model relating vehicle dynamics to current damage levels. Since it has been observed in the field that damage accumulates with the number of load repetitions, with the amount of damage also depending on temperature and the magnitude, configuration, and duration of loading, the response behaviour of these models must also be time-and temperature-dependent.

PAVEMENT CHARACTERIZATION

The response of a pavement structure in a given traffic and climatic environment has been divided, for the purposes of this analysis, into the primary and ultimate response modes. The ultimate response mode includes both damage (rutting, cracking, etc.,) and serviceability.

1 Center for Construction Research and Education, Department of Civil Engineering, Massachusetts Institute of Technology, Cambridge

In most cases, linear and non-linear materials are combined in pavement structures in such a way that the response of the structures to mechanical loadings may be described by linear equations. We will, therefore, describe the pavement response as a linear system, which may be defined as one whose mechanical behaviour can be represented by a set of linear differential or integral equations which are directly proportional to the magnitude of the applied load. When the structure can be considered as a linear system, its response to a general time-dependent load may be evaluated from its response to a step loading of unit magnitude (4).

The previous discussion applies to all pavements; however, in this paper, we will limit our analysis to flexible pavements, since the boundary condition, geometry, and loading patterns are easier to characterize for these pavements than for rigid pavements. We modeled pavement responses to moving, dynamic vehicle loads using a modified version of the VESYS IIIA flexible pavement model (5).

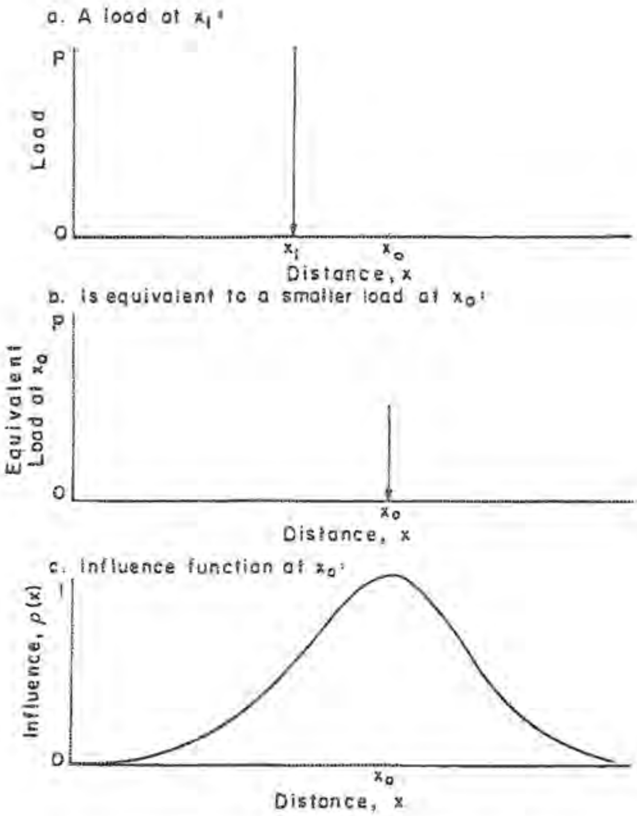

Load influence representation of a deterministic moving load

FIGURE 1

LOAD CHARACTERIZATION

Pavements are subjected to both traffic and environmental loads. While our primary focus in this research is on traffic loads, environmental loads must also be considered for the following reasons:

1. Environmental loads produce primary responses (i.e., stresses, strains, and deflections) in the pavement structure similar to those produced by vehicle loads; and

2. Environmental variations alter the layer materials properties, affecting both the primary and ultimate responses produced by vehicle loads.

To clarify the effects of the various types of traffic loading conditions, we assume for the following discussion that the environment is constant (i.e., effect (2) is present but unchanging) and such that effect (1) is negligible compared to the load-induced primary responses.

For a deterministic stationary load, the pavement primary response may be obtained by multiplying

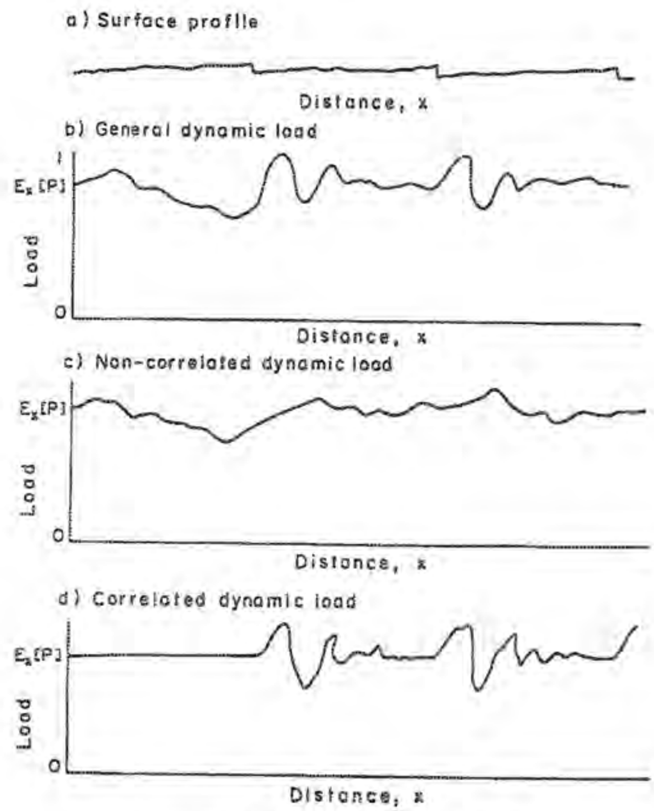

Types of dynamic loading

FIGURE 2

the response to a step loading of unit magnitude by the tire contact pressure, due to the linearity of the system. A deterministic moving load may be modeled as a footprint of uniform contact pressure moving at a constant velocity V in a straight line along the longitudinal direction of the pavement structure. It is often further assumed that the load will pass directly over the point of interest (x_o). The response at the point of interest will increase as the load approaches and decreases as the load moves away. If the system is elastic, the peak response will occur when the load is directly overhead; in the viscoelastic case, the peak response occurs slightly after the load has passed directly overhead (6).

The calculation of pavement responses to different representations of vehicle loadings, including a moving, dynamic load, is reviewed in reference (7). It may be demonstrated that, for credible highway vehicle speeds, the inertial response of a pavement to a moving load is negligibly small. Thus, we may treat the deterministic moving load case as a quasi-static problem.

THE INFLUENCE FUNCTION

For a linear system, the pavement response to a moving load may be calculated using an "approximate" moving load response wherein the load footprint is assumed to be always above the point of interest, but the contact pressure varies with time to reflect the approaching and passing away of the load. This transforms the "movement" of the load from space and time to time only. That is, the pavement response to a load at a distance is replaced by the response to a smaller load placed directly above the point of interest (Figure 1).

To represent this effect analytically, we use an influence function$\rho(x)$, which is normalized at x_o (Figure 1c). For example, the load influence at x_o of a load P placed at x_1 (and hence the pavement response to that load) is given by:

$$I(x_o) = P \bullet \rho(x_1 - x_o) \qquad (1)$$

where

$I(x_o)$ = load influence at x;

P = load at x_1;

$\rho\ (x_1 - x_o)$ = influence function at x.

For an elastic system, the peak influence (peak pavement response) occurs at x_o, and the influence function is symmetrical about x_o. The influence function differs by pavement design, season, pavement response parameter, pavement layer, and load radius. Influence functions become broader with stiffer pavements or with increasing pavement depth. The influence functions for a given pavement, season, and radius of load may be generated by applying a static load at x_o and calculating the desired pavement responses for a vector of points:

$$\rho(x_i - x_o) = \frac{R_i}{R_o} \qquad (2)$$

where x_i = point at which the influence function is required; R_i = pavement primary response at x_i; R_o = pavement primary response at x_o.

PAVEMENT RESPONSE TO A MOVING, DYNAMIC LOAD

A moving, dynamic vehicle load may be defined as a moving load which varies as a function of distance (or time) about a mean value. Two specific types of vehicle dynamic loading, which are produced by two different types of pavement roughness excitation, should be considered:

1. Randomly distributed surface roughness induces a stochastic pattern of vehicle dynamic responses. There is no preferred location to sample such a loading pattern, and the loading statistics are the same for every pavement location. This loading may be modeled by assuming a stochastic loading model which is not correlated with specific points of the pavement surface profile. Such a loading is shown in Figure 2c.

2. Certain specific pavement surface features, such as faulted rigid pavement joints, produce strong vehicle responses. The expected vehicle dynamic loading becomes highly dependent on the sampling location. Thus, in modeling these loading patterns, the loading statistics should be correlated with specific pavement surface roughness features (see Figure 2d).

In general, vehicle dynamic loading is composed of both stochastic and location-dependent components, which may be decoupled and analyzed separately. For flexible pavements, however, vehicle dynamic loading may be assumed to be dominated by stochastic loading, and thus vehicle loading and pavement response may both be treated stochastically. For rigid pavements location-dependent dynamic loadings produced by faulted joints and cracks will substantially affect pavement responses and must be considered.

The pavement response to a moving, dynamic load may be computed by multiplying the dynamic load by the influence function at the point of interest. Equation (1) becomes:

$$I(x_o) = P(x_1)\,\rho\,(x_1 - x_o) \qquad (3)$$

where $P(x_1)$ = instantaneous vehicle dynamic load at x_1; and other variables are as previously defined.

PAVEMENT RESPONSE TO REPEATED MOVING, DYNAMIC LOADS

The pavement response to a sequence of moving loads reflects the interaction between the primary response and ultimate response models. This is most often represented as a one-way interaction, wherein the primary responses affect the ultimate responses, but not vice-versa. The simplest such interaction is that where the moving loads, and hence the primary responses, are all identical. In this case, the ultimate response (cumulative damage) may be expressed in terms of the peak primary response to a single moving load and the number of load applications (4,6).

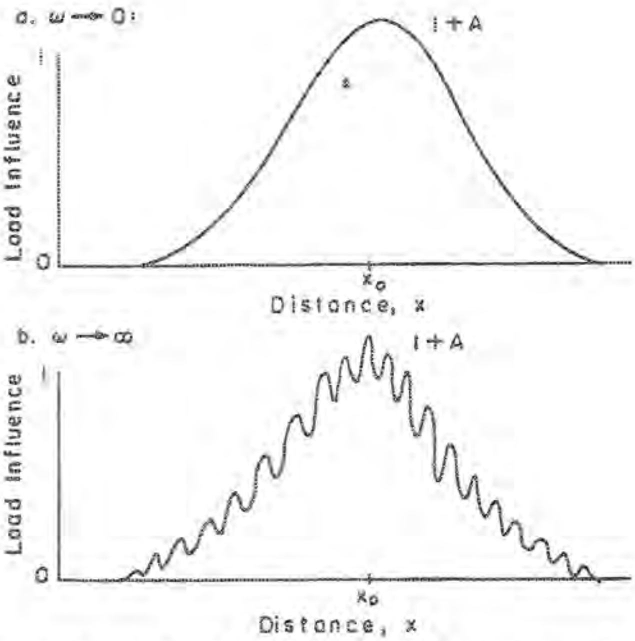

Variation in load influence with frequency of load oscillations, for special case of zero phase angle

FIGURE 3

The peak primary response at x_o, is, of course produced by the peak load influence at x_o. The cumulative damage functions are different for each pavement response parameter (i.e., rutting or cracking). Prior to our modification, the VESYS IIIA cumulative damage models used the mean and variance of loading of the traffic stream as inputs. We replaced these with the mean and variance of the peak influence.

To examine the behaviour of a flexible pavement under repeated vehicle dynamic loading, let us consider an idealized sinusoidal single axle loading:

$$P(x) = 1 + A\cos(\omega x + \phi) \qquad (4)$$

where $P(x)$ = normalized instantaneous axle load at point x; A = amplitude of sinusoidal load variation, as a fraction of $\overline{P}$; ω = frequency of load variation; x = distance; ϕ = phase angle.

The peak influence becomes:

$$I(x_o, \phi) = \text{Max}\,[(1 + A\cos(\omega x + \phi))\,\rho\,(x_o - x)] \qquad (5)$$

where all variables are as previously defined. ϕ is considered random, and is varied from 0 to 2π (and $I(x_o, \phi)$ is averaged over ϕ), to represent the non-correlated vehicle dynamic loading model.

Two limiting values of ω should be considered;

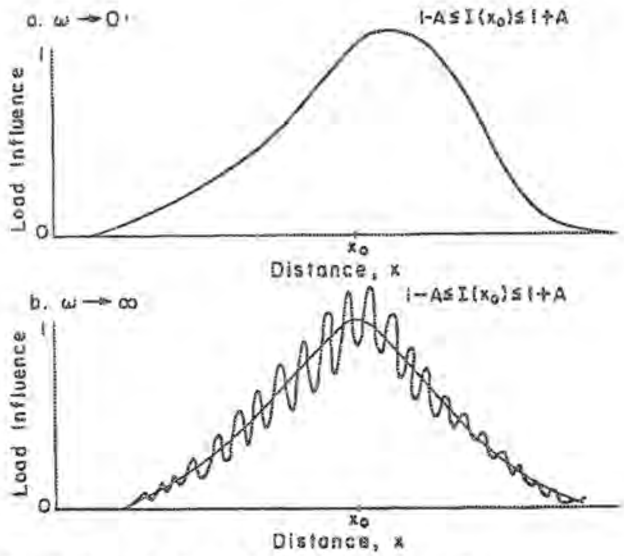

Variation in load influence with frequency of load oscillations, for general case of zero phase angle

FIGURE 4

1. At $\omega = 0$, equation (5) becomes:

$$I(x_o, \phi) = [1 + A \cos(\phi)] \quad (6)$$

Note that Max $[\rho(x_o - x)] = 1$. Since is ϕ random, in this case $E[I(x_o, \phi)]$ equals 1, and σ_I^2 equals σ_P^2 which equals $A^2/2$. Figures 3a and 4a show the influence of a sinusoidally varying load with a very small ω. Depending on ϕ, max $[I(x_o, \phi)]$ may occur some distance from x_o and is almost as equally likely to be less than 1 as it is to be greater than 1. Consequently, the mean peak influence is close to 1 and the variance is high.

2. As ω approaches ∞, equation (5) becomes:

$$I(x_o, \phi) = 1 + A \quad (7)$$

Since $\cos(\infty)$ can take any value, Max $[(\cos(\infty)] = 1$. $E[I(x)]$ equals $\bar{P}[1 + A]$, and $\sigma_I^2 = 0$. To illustrate this, Figures 3b and 4b show the influence of a sinusoidally varying loading with a very large ω. It may be seen that for any value of ϕ the peak influence will be located very close to x_o, and its value will be very close to 1+A. The mean peak influence is approximately equal to 1+A and the variance is small.

For intermediate values of ω, $E[I(xo, \phi)]$varies from 1 to 1+A, and σ_I^2varies from 0 to σ_P^2. Therefore, the statistics of the peak load influence vary from the statistics of loading ($\bar{P}$ and σ_P^2) in two ways (for all $\omega > 0$):

1. The mean peak influence is greater than the mean peak load.

2. The variance of the peak influence is less than the variance of the load.

Many vibrational modes contribute to vehicle dynamic behaviour. In the MIT vehicle model (see Part I of this paper), this is represented by means of masses, linear and non-linear springs, and damping. The pavement roughness exciting the vehicle model is random. As a result, the P(x) profiles provided by the vehicle model are complex and non-periodic.

The effect of these P(x) profiles on I(x), however, is the same as that of the sine wave model just reviewed. They increase the mean peak influence over the mean dynamic load and produce a variance of the peak influence which is less than the variance of the load. As a result, in the interfacing of the vehicle and pavement models the representation of dynamic loading used must reproduce the peak influence statistics computed with the vehicle dynamic loading history. This suggests that it may be possible to approximate dynamic loading in such a manner that these statistics may be computed without actually using the dynamic loading history.

We investigate the possibility of using a periodic model, such as a Fourier series, or a statistical model, such as an autocorrelation function, to represent dynamic loading, as reviewed in reference (7). However, none of these models proved satisfactory, so we used a digitized load profile generated by the MIT vehicle model to calculate the peak influence statistics. We calculated the peak influence statistics for a single dynamic loading profile as a function of distance, using the variation of dynamic loading of a single vehicle with distance to represent the variation of loading of a fleet of nominally identical vehicles at a single representative point of interest. The algorithm used is described in reference (7).

Changes to VESYS IIIA

Three sets of modifications were required to allow us to simulate flexible pavement responses to moving, dynamic single axle loads.

1. Representation of dynamic loads: Influence functions must be generated (using a static load analysis) and stored for each required primary response parameter, radius and season. The vehicle dynamic load profile generated by the MIT vehicle model (see Part I of this paper), is then multiplied by the influence function at each sampling interval to obtain the dynamic load-pavement interaction factors (E(I(x)) and), which are used to calculate damage. Since these factors are different for each pavement layer, rutting is calculated for each pavement layer rather than for the pavement structure as a whole, as in the previous version of VESYS IIIA.

2. Relational modifications: The previous second order probabilistic damage relations were extended to fourth order probabilistic relations. The variation in the Miner's exponent for fatigue cracking was set to zero, since this variation had an unrealistically high impact on fatigue damage. An initial slope variance of 1.72×10^{-6} was assumed for a newly constructed pavement with an initial PSI of 4.2, using the following serviceability equation (8).

$$PSI = 5.03 - 1.91 \log(1 + SV) - 0.01\sqrt{C + P} - 1.38\,RD^2 \quad (8)$$

where PSI = present serviceability index; SV = slope variance x 10^6; C, P = areal cracking and patching, respectively, both measured in square feet per 1000 square feet; RD = rut depth, in. (2.54 cm); and setting C = P = RD = 0. Since the previous PSI model used in VESYS IIIA had assumed PSI = 4.2 at SV = 0, it was necessary to introduce a slope variance mapping factor (2.72) to calibrate equation (8) to the previous model.

3. Program structural modifications: In the previous version, the radius of the tire loading contact patch was input; we modified the program to calculate the radius from the total (half-axle) load and tire contact pressure. Pavement primary responses are computed for 3 radii, and results are parabolically interpolated for a specific radius. The vehicle dynamic load profiles are input by axle group. Axle equivalencies are automatically computated by damage type.

The pavement response parameters for permanent deformation (rutting) were changed from surface deflection, which was used in VESYS IIIA, to elastic compression in each pavement layer; for the subgrade, both deflection and maximum strain are used in the pavement response models (see multi-axle section, below). The rutting coefficients were made strain-dependent.

PAVEMENT RESPONSE TO REPEATED MOVING, DYNAMIC MULTIPLE AXLE LOADS

Tandems, tridems, and other multiple axles are designed to reduce pavement damage by distributing their loads over a larger area of pavement. Pavement responses to these axles are, in general, more complex than responses to single axles. The dynamic loads produced by multiple axles on flexible pavements are of interest for two reasons:

1. Vehicles with one or more multiple axles constitute the majority of modern heavy truck traffic (9).

2. Several previous studies of vehicular dynamic loading have focused on multiple axles (1,2,10). Modeling these axles makes it possible to relate our work to this previous research.

Multiple axles interact with each other, and thus the axle group must be analyzed as a whole and not as a series of independent loads. Axles interact only if the axle spacing (s) is less than a certain value, which is determined by the length of the influence function for the pavement on which the load is imposed and the response parameter under consideration. If one axle load is at x1 and the second is at x2, the loads interact if

$$\rho\,|\,s\,| = \rho\,|\,x_2 - x_1\,| > 0.$$

For a linear system the responses may be superimposed, as shown in Figure 5. This figure shows the pavement response (and load influence) produced by a stationary, deterministic tandem axle with two loads of equal magnitude and an axle spacing of s = 4.84 ft. (1.47 m). The solid line (Figure 5c) shows the sum of the load influences (11,12).

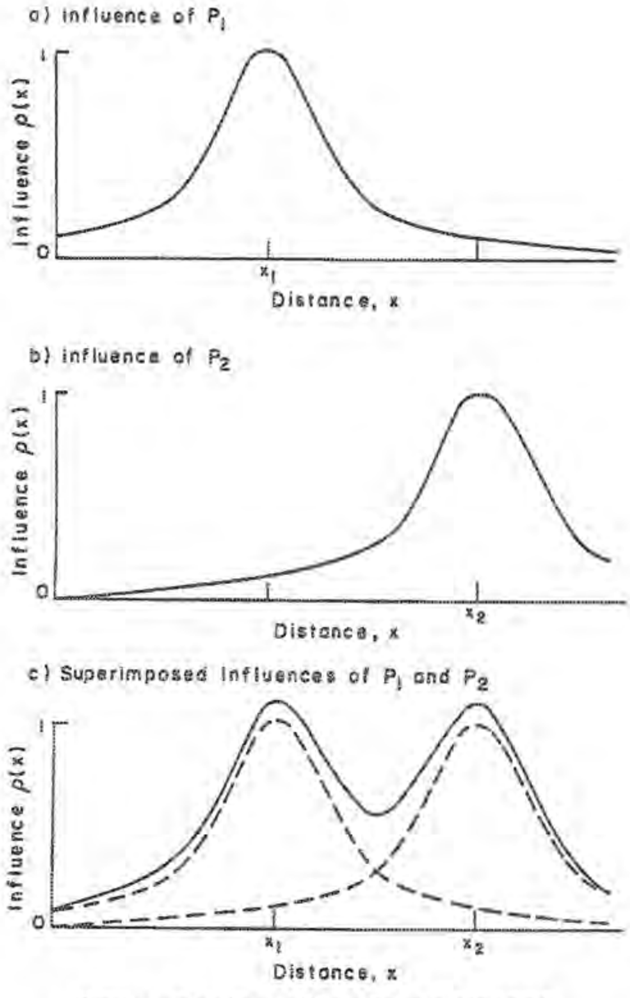

Superposition of tandem axle load responses (11, 12)

FIGURE 5

It may be seen that the load influence produced by a tandem axle is characterized by two maximum influences (I_1 and I_3) and one minimum influence (I_2). The influence of the tandem load may be modeled as two axle influences, one of magnitude I_1, and a second of magnitude I_4 ($I_4 = I_3 - I_2$), as shown in Figure 6. For an n-axle group, the load influence is characterized by n maximum influences and n-1 minimum influences, as shown in Figure 7 for a 3-axle group (tridem). The n-axle group may be modeled as a series of n load influences (Figure 7), calculated in the same manner as for tandems.

The damage caused by an axle group is dependent on the ability of the group to distribute loads evenly among its axles. For example, if the mean axle load of the first axle of a tandem is higher than that of the second axle, the increase in damage caused by the increased mean load of the first axle will more than compensate for the reduction in the damage produced by the second axle. Consequently, the tandem group will be more damaging. Sweatman (1) defined a Load Sharing Coefficient (LSC) to characterize this effect:

$$LSC = 2n\bar{P}/W \quad (9)$$

where n = number of axles in group; $\bar{P}$ = mean wheel force (kips or kN): W = axle group weight (kips or kN, same units as P).

Sweatman found that, in general, the rear axle of a tandem carries more than half of the total mean dynamic axle load. The LSC is dependent on vehicle suspension type, tire pressure, speed, and road roughness.

The pavement damage caused by moving, dynamic loads is influenced by the correlation between the axle loads as well as by load sharing. For example, if the axles of a tandem are in phase (if P_2 is high when P_1 is high), then the contribution of P_2 to the peak influence of P_1 is high. If, on the other hand, P_1 and P_2 are out of phase, the contribution of P_2 to the peak influence of P_1 is less, and pavement damage is reduced.

The correlation among multiple axle dynamic loads depends on the relative contributions of the various modes of vehicle behaviour. For example, the dynamic loadings produced by the vehicle

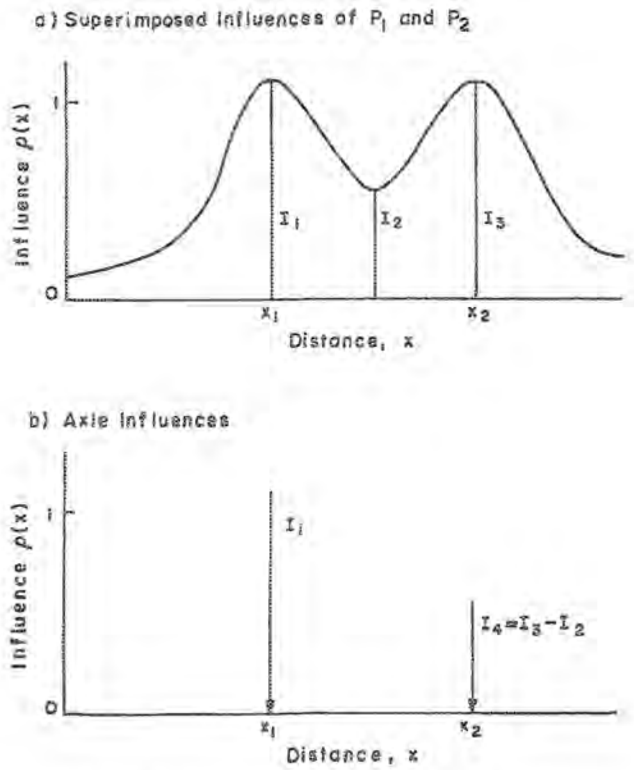

Load influence representation of a tandem axle load (11)
FIGURE 6

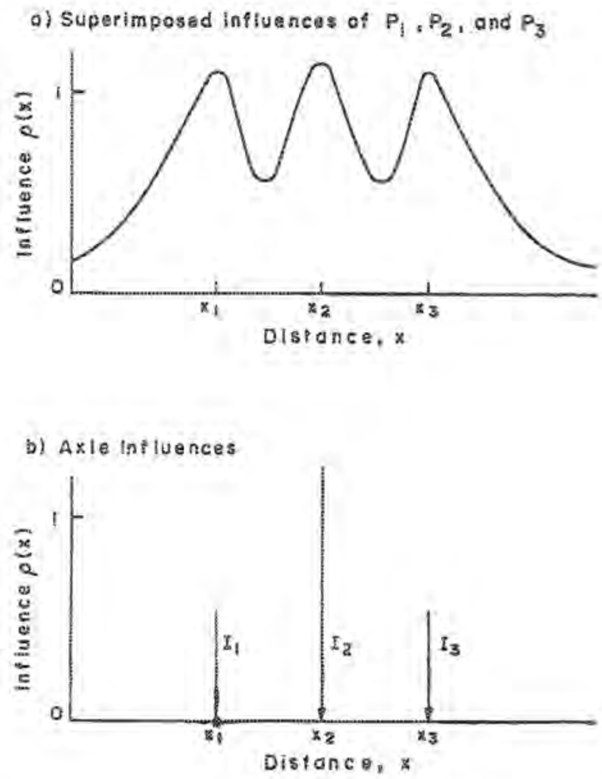

Load influence representation of a tridem axle load
FIGURE 7

body mode (~ 1 Hz) may be expected to be highly correlated, while the loadings produced by the wheel/suspension mode (~ 10 Hz) may be correlated, uncorrelated, or anticorrelated depending on the characteristics of the vehicle suspension.

Multiple axle dynamic loading is thus characterized by three components of behaviour:

1. Distribution of the mean dynamic load among axles (characterized by the LSC);
2. The variation of dynamic loading for each axle (characterized by a DLC (see Part I of this paper) or by frequencies and corresponding amplitudes of axle vibration) for each axle;
3. The correlation of the individual axle dynamic loads with each other.

MODIFICATION OF THE VESYS IIIA RUTTING MODEL FOR MULTIPLE AXLE LOADS

For single axles our rutting model gave excellent results. However, when the model was applied to tandem axles, rutting was much higher than that which would be expected on the basis of the AASHO Road Test results. Further investigation indicated that the overprediction of rutting was occurring in the subgrade.

While the compressive stresses and strains at the top of the subgrade are less for a tandem axle than for a single axle with the same total axle load, the subgrade deflections may be almost as great for the tandem, particularly under a stiff pavement. This indicates that the benefit of a multiple axle in reducing pavement damage lies in the reduction of compressive stresses and strains, since the reduction of total deflection may be small. The compressive strain at the top of the subgrade has been used as a criterion for pavement design to prevent excessive rutting (13) and has been used to calculate mechanistic axle equivalencies for single and multiple axles (12). Thus it seems logical to base rutting on the maximum compressive stress or strain at the top of the subgrade.

Rutting is caused by the accumulation of permanent strain within a pavement structure. For paving materials permanent strain may be predicted from elastic strain:

$$\varepsilon_p = \varepsilon \mu N^{\alpha} \qquad (10)$$

where ε_p = permanent strain; ε = elastic strain; N = number of repetitions of the elastic strain (load repetitions); = μ, α materials parameters.

Note that for a multiple, n-axle load, there are n load pulses, each of which is characterized by a peak compressive strain. The following discussion applies to all load pulses.

For a finite pavement layer, total permanent layer deformation may be calculated from permanent strains:

$$R_p = h\,\overline{\varepsilon_p} = h\,\overline{\mu\varepsilon}\,N^{\alpha} \qquad (11)$$

where R = permanent layer compression; h = thickness of layer; $\overline{\varepsilon_p}$ = average permanent strain; ε = average elastic strain.

Total rutting for the pavement structure becomes:

$$R_{pt} = \sum_{i=1}^{n} R_{pi} \qquad (12)$$

where R_{pt} = total rutting; i = layer number; n = number of layers; R_{pi} = permanent compression of layer i.

For an infinite layer, that is, the subgrade, equation 911) cannot be used to predict rutting, since $h = \infty$ and $\overline{\varepsilon_p} = 0$. Consequently, the original VESYS IIIA rutting model used deflection to predict rutting in the subgrade:

$$R_p = \delta \mu \ \ N^{\alpha} \qquad (13)$$

where δ = subgrade deflection = $\int_{h_1}^{\infty} \varepsilon\, dz$;

h_1 = depth to the top of the subgrade.

In order to create a strain-based rutting model, we shall assume that all of the rutting in the subgrade occurs within a finite depth. The subgrade material below this depth may be assumed to be either perfectly rigid or linearly elastic (in actuality, the stresses are so low that there is no permanent deformation in this material). The subgrade may be treated as a layer of thickness h', and equation (11) may be applied.

We further assumed that the average compressive strain ε may be related to the peak compressive strain at the top of the subgrade through a proportionality constant k:

$$k = \frac{\bar{\varepsilon}}{\varepsilon_{max}} \tag{14}$$

where ε_{max} = maximum compressive strain at the top of the subgrade due to a primary or secondary peak.

Equation (11) then becomes:

$$Rp = h' \ \mu \ k\varepsilon_{max} N^{\alpha} \tag{15}$$

The product h′ k may be evaluated by using equation (13) for single axles, since this equation predicts rutting well for these axles. Setting equation (13) equal to equation (15), we may calculate h′ k:

$$h' k = \frac{\delta_s}{\varepsilon_s} \tag{16}$$

where δ_s = deflection produced by a single axle; ε_s = peak subgrade compressive strain produced by a single axle.

Equation (15) becomes:

$$R_p = m \ \frac{\delta_s}{\varepsilon_s} \ \varepsilon_{m,n} \ N^{\alpha} \tag{17}$$

where $\varepsilon_{m,n}$ = peak subgrade compressive strain produced by the nth load pulse of a multiple axle group and other variables are as previously defined.

This multiple axle rutting model was added to VESYS IIIA.

Table 1 – AASHO flexible pavement sections modeled

Design number	Structural number	Section	Number of axle loads (in kips)
3-3-8	2.62	3	12, 18, 22.4
5-3-8	3.50	6	18, 22.4, 30 single 32, 40, 48 tandem
4-6-12	3.92	6	18, 22.4, 30 single 32,40,48 tandem
5-6-12	4.36	8	18, 22.4, 30 single 32, 40, 48 tandem
Total =		23	

VERIFICATION: SIMULATING THE AASHO ROAD TEST

To test the flexible pavement model of dynamic loads, we simulated selected pavements of the AASHO Road Test. The Road Test was well-documented, and as a result we had at our disposal substantial data on the vehicles, pavements, environment, and damage and serviceability measurements (8,14). These data had been used by the Federal Highway Administration (FHWA) to validate VESYS IV for single axles on flexible pavements. In the FHWA study, nineteen sections from the Road Test were modeled (14). We used the VESYS data sets from the FHWA to model 23 of these sections (see Table 1).

Pavements

The 23 pavements simulated represent four different flexible pavement designs, summarized in Table 1. The design numbers refer to thickness (in inches, 1 in. = 2.54 cm) of surface course, base course, and subbase course, respectively. The layer materials used in all designs were identical.

Vehicles

In these trials we simulated loads of 12, 18, 22.4, and 30 kip (53.3, 80, 99.5, and 133.2 kN, respectively) single axles and 32, 40, and 48 kip (142.1, 177.6 and 213.1 kN, respectively tandems). Each Road Test vehicle had one 4, 6, 9, or 12 kip (17.8, 26.7, 40, or 53.3 kN, respectively) steering axle and two load axles (15).

Environment

Vehicle load application at the Road Test began on October 15, 1958, and ended November 30, 1960, an interval encompassing eight seasons. During this time, 1,114,000 axle load applications were made, at a rate of 800 to 2,356 axles per day, providing an accelerated loading of the pavement test sections.

Vehicle loads are more damaging at certain times of the year, particularly during the Spring thaw. Most Road Test pavements failed in either Spring 1959 or Spring 1960. At other times of the year, such as during Winter, loads had almost no effect. To account for this, weekly weighing factors based on pavement deflections on an untraveled control loop, were calculated to account for environmental factors. The weighing factors, varying from 0 to 4.84, were multiplied by the number of axle applications for that week, yielding a weighted axle application number for that week (8).

We used the following approximate seasonal weighing factors (based on four seasons of equal length):

- Winter 0.36 (the AASHO Road Test began in October)
- Spring 1.91
- Summer 1.26
- Fall 0.81

COMPARISON OF DAMAGE AND SERVICEABILITY PREDICTIONS

For the 13 AASHO single axle flexible pavement sections modeled (see Table 1), comparisons were made of rut depth, slope variance, cracking, and serviceability (PSI) among (1) the damage traces of the AASHO Road Test, (2) VESYS predictions by the FHWA (14), and (3) our results (both with and without dynamic vehicle loading). The VESYS damage predictions presented by the FHWA in reference (14) were based on VESYS IV; we used the same data sets and an earlier version of VESYS IIIA (modified for dynamic loads).

Comparisons between modified VESYS IIIA dynamic predictions and the Road Test damage traces versus unweighted axle repetitions for 8 of these sections are reported in reference (7). For two single axle sections, these comparisons are plotted in Figure 8 and 9. The modified VESYS IIIA plotted predictions represent mean dynamic results.

In general, our damage and serviceability predictions were very good. The predictions fit the Road Test data both in the character of the damage patterns and, in most cases, the magnitude of the damage.

For the AASHO tandem axle sections, damage traces were not available, so we were limited to

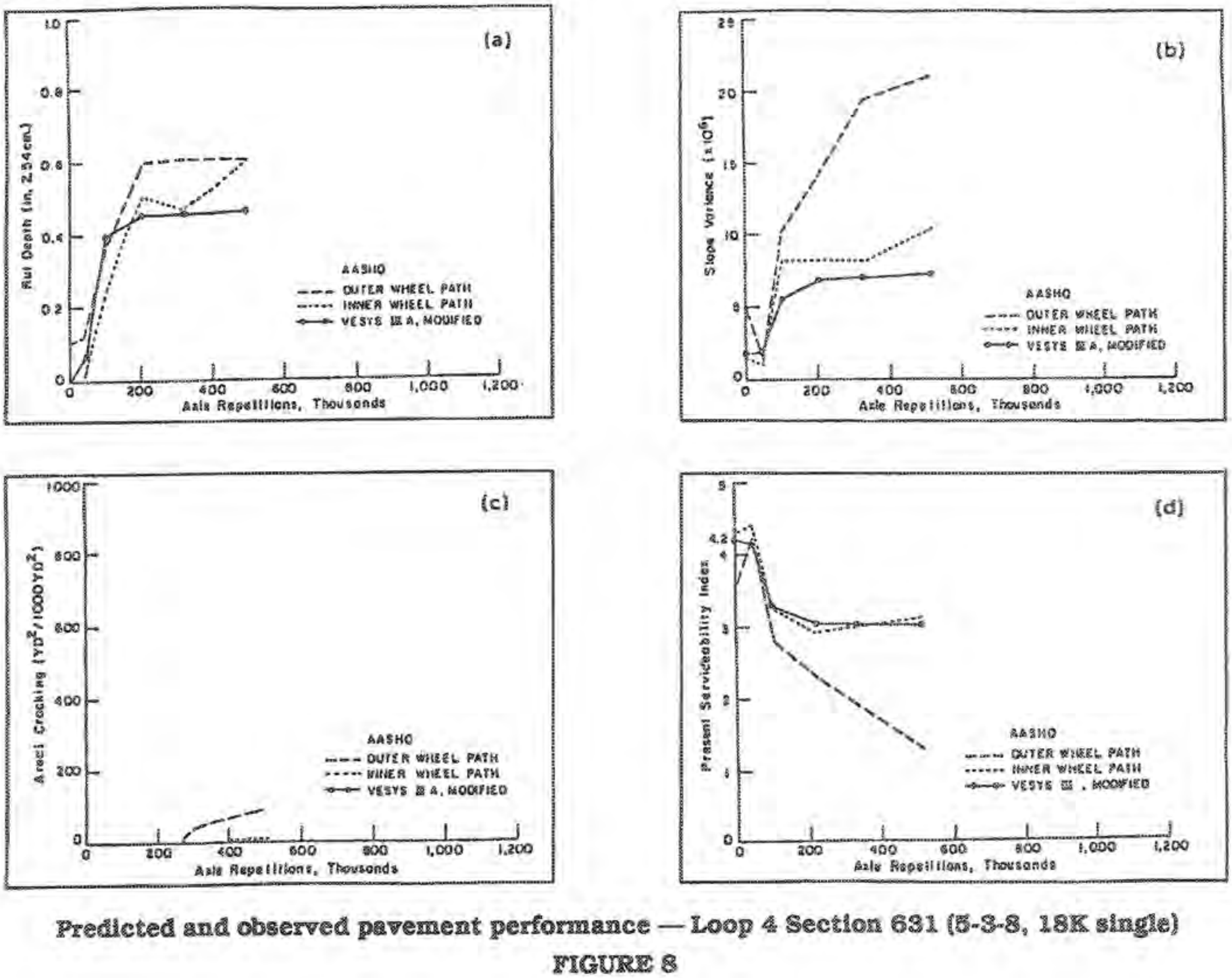

Predicted and observed pavement performance — Loop 4 Section 631 (5-3-8, 18K single)

FIGURE 8

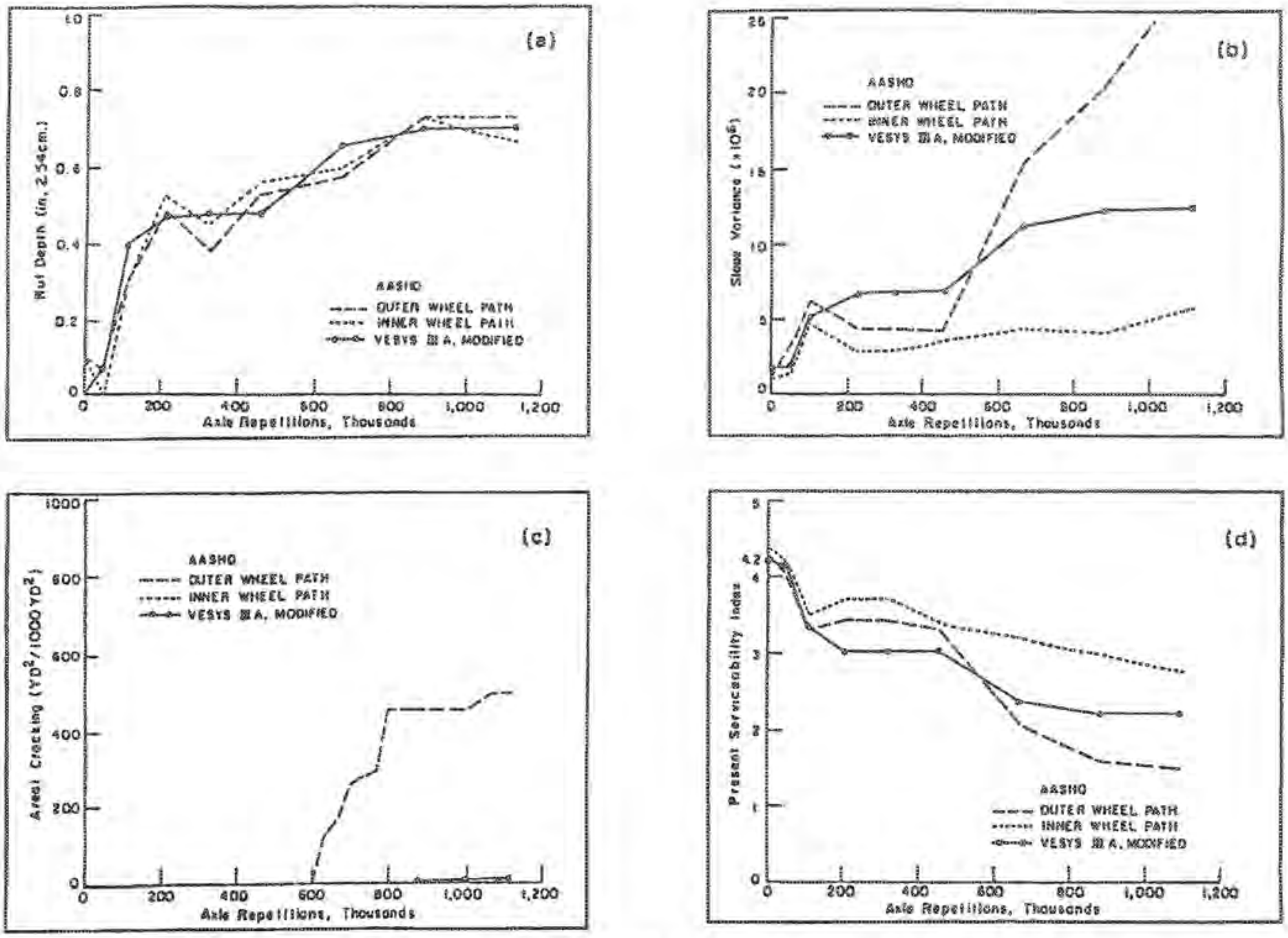

Predicted and observed pavement performance — Loop 5 Section 445 (5-6-12, 22.4K single)

FIGURE 9

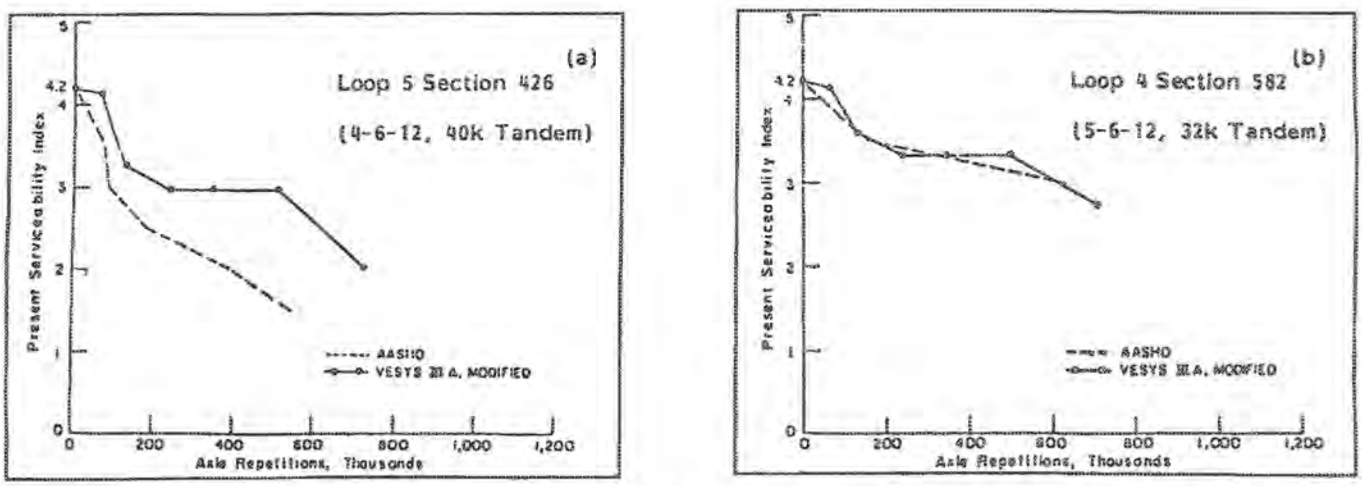

Predicted and observed serviceability for various tandem axle sections

FIGURE 10

comparing serviceability predictions and data (8). (Four comparisons, one including the two replicate sections, are plotted in Figure 10.) A more complete report of our tandem axle results is given in reference (7). Again, strong correlation was found between the AASHO results and our predictions.

SUMMARY AND RECOMMENDATIONS FOR FUTURE RESEARCH

In this paper we have developed a method for the analysis of the effects of repeated moving, dynamic vehicle loads on highway pavements.

The method has been verified through a simulation of pavement performance data gathered during the AASHO Road Test (8,14). For all of the pavements analyzed, our model produced reasonable results.

This paper is reporting on work in progress; in the final year of the project we will work to extend the model to rigid pavements. We will also consider a wider range of vehicle types and vehicle parameters, as suggested in Part I of this paper.

REFERENCES

1. Sweatman, P. F. "A Study of Dynamic Wheel Forces in Axle Group Suspensions of Heavy Vehicles," Australian Road Research Board Special Report No. 27.*

2. Whittemore, A.P., Wiley, J.R., Schultz, P.C., and Pollock, Donald E. Dynamic Pavement Loads of Heavy Highway Vehicles, National Cooperative Highway Research Program Report 105, Highway Research Board, 1970.

3. Ullditz, P., and Larsen, B.K. "Mathematical Model for Predicting Pavement Performance," pp. 45-55, Transportation Research Record No. 949, Transportation Research Board, National Academy of Sciences, 1984.

4. Moavenzadeh, F., and Elliott, J.F. "Moving Load on a Visco-elastic Layered System," MIT CE Report No. R68-37, June, 1968.

5. Kenis, William J. "Predictive Design Procedure--A Design Method for Flexible Pavements Using the VESYS Structural Subsystem," Proceedings, Fourth International Conference on the Structural Design of Asphalt Pavements, 1977.

6. Elliott, J.F., and Moavenzadeh, F. "Moving Load on a Visco-elastic Layered System, Phase II," MIT CE Report No. R69-64, September 1969.

7. Delatte, N. J. "Characterization of Dynamic Vehicle-Pavement Interactions," Thesis presented to the Massachusetts Institute of Technology, in partial fulfillment of the requirements for the degree of Master of Science, 1986.

8. The AASHO Road Test, Report 5, "Pavement Research," Highway Research Board Special Report 61E, National Academy of Sciences, National Research Council Publication 954.

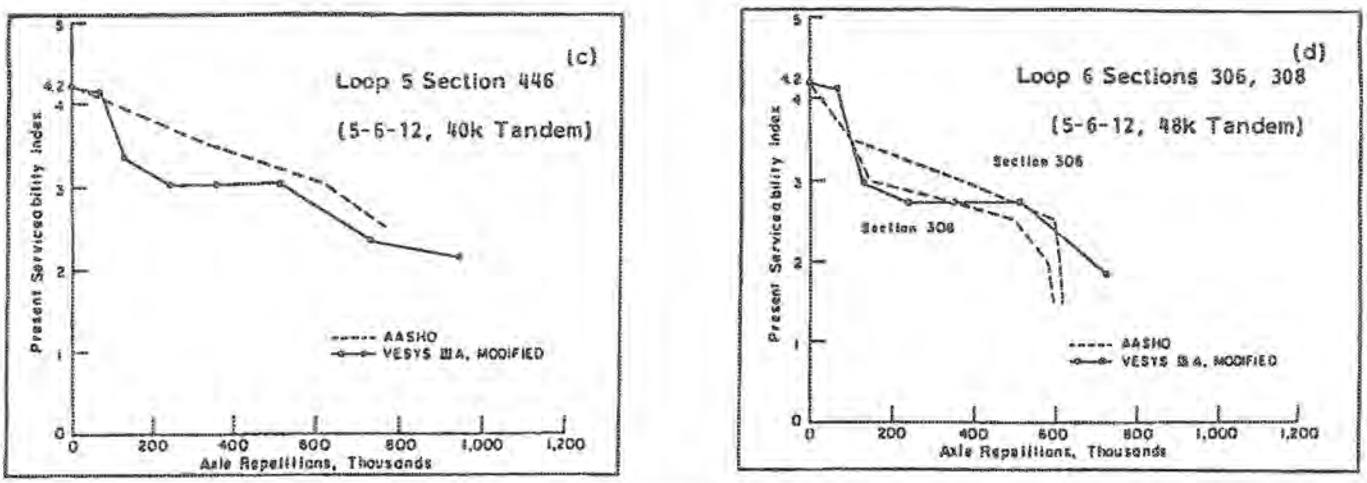

Predicted and observed serviceability for various tandem axle sections

FIGURE 10

9. Middleton, Dan R., Roberts, Freddy, L., and Chira-Chavala, T. Measurement and Analysis of Truck Tire Pressures on Texas Highways, The Texas Transportation Institute, Texas A&M University, January 1986.

10. Treybig, H.J. "Equivalency Factor Development for Multiple Axle Configurations," p. 32, Transportation Research Record No. 949, Transportation Research Board, National Academy of Sciences, 1984.

11. Rauhut, J.B., Lytton, R.L., and Darter, M.I. "Pavement Damage Functions for Cost Allocation," Vol. II, Descriptions of Detailed Studies, Report FHWA/RD-84/019, June, 1984.

12. Wang, M.C., and Anderson, R.P. "Load Equivalency Factors of Loading for Flexible Pavement," p. 42, Transportation Research Record No. 810, Transportation Research Board, National Academy of Sciences, 1981.

13. Majidzadeh, K., Bayomy, F., and Khedr, S. "Rutting Evaluation of Subgrade Soils in Ohio," pp. 75-84, Transportation Research Record No. 671, Transportation Research Board, 1978.

14. Kenis, W.J., Sherwood, J.A., and McMahon, T.F. "Verification and Application of the VESYS Structural Subsystem," Proceedings, Fifth International Conference on the Structural Design of Asphalt Pavements, Volume I, 1982.

15. The AASHO Road Test, Report 5, "Traffic Operations and Pavement Maintenance," Highway Research Board Special Report 61E, National Academy of Sciences, National Research Council Publication 952.

SESSION 10
TECHNO-ECONOMIC IMPACT OF REGULATORY MEASURES

Chairman:

B. Guey
Western Highway Institute
United States